

## Research Article

# Adsorption of Hg(II) from Aqueous Solution Using Adulsa (*Justicia adhatoda*) Leaves Powder: Kinetic and Equilibrium Studies

Mohd Aslam,<sup>1,2</sup> Sumbul Rais,<sup>2</sup> Masood Alam,<sup>2</sup> and Arulazhagan Pugazhendi<sup>1</sup>

<sup>1</sup> Center of Excellence in Environmental Studies, King Abdulaziz University, Jeddah 21589, Saudi Arabia

<sup>2</sup> Department of Applied Sciences and Humanities, Faculty of Engineering and Technology, Jamia Millia Islamia, New Delhi-110025, India

Correspondence should be addressed to Mohd Aslam; [aslam312@gmail.com](mailto:aslam312@gmail.com)

Received 9 May 2013; Revised 16 July 2013; Accepted 18 July 2013

Academic Editor: Nurettin Sahiner

Copyright © 2013 Mohd Aslam et al. This is an open access article distributed under the Creative Commons Attribution License, which permits unrestricted use, distribution, and reproduction in any medium, provided the original work is properly cited.

The ability of Adulsa leaves powder (ALP) to adsorb Hg(II) from aqueous solutions has been investigated through batch experiments. The ALP biomass was characterized by Fourier transform infrared spectroscopy and scanning electron microscopy. The experimental parameters that were investigated in this study included pH, adsorbent dosage, and effect of contact time along with initial metal ion concentration. The adsorption process was relatively fast, and equilibrium was achieved after 40 min of contact time. The maximum removal of Hg(II), 97.5% was observed at pH 6. The adsorption data were correlated with Langmuir, Freundlich, and Temkin isotherms. Isotherms results were amply fitted by the Langmuir model determining a monolayer maximum adsorption capacity ( $q_m$ ) of ALP biomass equal to  $107.5 \text{ mg g}^{-1}$  and suggesting a functional group-limited sorption process. The kinetic process of Hg(II) adsorption onto ALP biomass was tested by applying pseudofirst-order, pseudosecond-order, Elovich, and intraparticle-diffusion models to correlate the experimental data and to determine the kinetic parameters. It was found that the pseudosecond order kinetic model for Hg(II) adsorption fitted very well. The rate determining step is described by intraparticle diffusion model. These studies considered the possibility of using Adulsa plant leaves biomass as an inexpensive, efficient, and environmentally safe adsorbent for the treatment of Hg(II) contaminated wastewaters.

## 1. Introduction

The presence of toxic heavy metals in aqueous stream, arising from the discharge of untreated metal containing effluents into water bodies has become one of the most important environmental issues in the past few decades. Mercury is an element, and it cannot be created by people, nor can it be destroyed. Mercury is released into the environment by volcanic eruptions, and it naturally occurs in the earth's crust, often in the form of mercury salts such as mercury sulfide [1].

Mercury, amongst other heavy metals has attracted global concern due to its extensive use, toxicity, wide spread distribution, and the biomagnifications. Several kinds of human

activities (anthropogenic) release mercury into the environment that include effluents from paint and chloralkali, pulp paper, oil refining, battery production, fossil fuel burning, mining and metallurgical processes, rubber processing, and fertilizer industries [2–5]. Other major source of mercury emission into the atmosphere is flue gases from coal combustors used in electricity generation [6, 7]. The European Union considers mercury as a priority and hazardous pollutant and defines a maximum permissible concentration of total mercury as low as  $1 \mu\text{g L}^{-1}$  for drinking water and  $5 \mu\text{g L}^{-1}$  for wastewater discharge [8]. The primary targets for toxicity of mercury and mercury compounds are the nervous system, the kidneys, and the cardiovascular system.

It is generally accepted that developing organ systems (such as the fetal nervous system) are the most sensitive to toxic effects of mercury. Other systems that may be affected include the respiratory, gastrointestinal, hematologic, immune, and reproductive systems [9].

Conventional treatments to remove mercury from aqueous solution include precipitation, electrolysis, ion exchange, adsorption, cementation, liquid membranes, and liquid-liquid extraction [10, 11]. However, these processes are ineffective at low metal concentration or expensive due to toxic sludge disposal, chemical reagents for metal recovery, and sorbent regeneration and high energy requirements. Therefore, more effective low cost alternatives are urgently required. In the past two decades, biosorption received a considerable attention for the removal of heavy metals from waste water [12–17].

Various potentially inexpensive adsorbents such as bark [18], *Carica papaya* [19], Sewage sludge [20], wheat bran [21], walnut shell [22], coffee grounds [23], waste rubber [24], coconut husk [25], fertilizer waste slurry [26], algae [27], peanut hull [28], jackfruit peel [29], coal-fly ash [30], coir pith [31], and sago waste [32] have been used for the removal of mercury from aqueous solution.

*Adulsa (Justicia adhatoda)* is a small evergreen herbal plant in the family *Acanthaceae*. It is distributed all over the plains of India and in lower Himalayan ranges. The leaves of the plant contain an essential oil and alkaloids vasicine, N-oxides of vasicine, vasicinone, deoxyvasicine, and maiontone. The plant has been recommended by Ayurvedic physicians for the management of various types of respiratory disorders. It possesses potent bronchodilatory, expectorant, antispasmodic and antiseptic properties. The aim of the present study is to evaluate the potential of *Adulsa* leaves powder (ALP) biomass for the adsorption of mercury from aqueous solution by batch operation technique. The effects of optimum biosorption conditions such as pH, initial metal ion concentration, contact time, and biomass dosage have been explored. The Langmuir, Freundlich, and Temkin models were used to describe the equilibrium isotherms. To correlate the experimental data and to determine the kinetic parameters, pseudofirst order, pseudosecond-order, intraparticle diffusion, and Elovich model were evaluated.

## 2. Experimental

**2.1. Adsorbate Preparation.** The stock aqueous solutions of desired concentration have been prepared by dissolving the appropriate amount of  $\text{Hg}(\text{NO}_3)_2 \cdot \text{H}_2\text{O}$  in double distilled water (DDW). The stock solution was used to prepare dilute solutions of different working concentrations. All the chemicals used in this study were of analytical grade from Merck Company (Darmstadt, Germany).

**2.2. Adsorbent Preparation.** *Adulsa* leaves powder (ALP) used as an adsorbent were collected from Horticulture Department, Jamia Millia Islamia, Central University, New Delhi, India. The plants were washed thoroughly using tap water in order to remove the water soluble impurities and

other surface-adhered particles. Only the leaves of the plants were utilized in this study. The washed plant leaves were oven-dried at  $80^\circ\text{C}$ , ground using a blender and sieved through a 40–50 mesh BSS screens in order to obtain uniform particle size. Leaves biomass was washed four times with DDW in order to remove soluble material or biomolecules that might interact with any adsorbed metal ions. So obtained biomass was dried in oven at  $80^\circ\text{C}$  and stored in desiccators.

**2.3. Adsorbate Analysis.** The final solutions of mercury concentrations of the samples were determined by using a flow injection analysis system, atomic absorption spectrophotometer (FIAS-AAS, Perkin-Elmer model 3100). The analytical wavelength used was 253.7 nm with a slit width of 0.7 nm having hollow cathode lamp current of 6 mA current. Standards were prepared by diluting a 1000 mg/L  $\text{Hg}(\text{II})$  stock solution with 3% HCl solution and 2–3 drops of  $\text{KMnO}_4$ , and linear calibration curves were obtained with correlation coefficients of  $R^2 = 0.99$  or better. Three replicates of each sample were analyzed, and the mean value was reported.

**2.4. Batch Adsorption Studies.** The batch adsorption studies were carried out in 250 mL Erlenmeyer flasks containing 1 g of the adsorbent in 100 mL of  $\text{Hg}(\text{II})$  solution at  $30 \pm 2^\circ\text{C}$  on a rotary shaker at 150 rpm. The effect of pH on biosorption rate was investigated in a pH range of 3 to 9, which was regulated by microadditions of 0.1 N HCl or 0.1 N NaOH at the beginning of the experiment. The best amount of biomass was determined by changing the biomass dosage from 0.25 g to 1 g in 100 mL of  $\text{Hg}(\text{II})$  solution. The initial concentration of  $\text{Hg}(\text{II})$  solution taken for this study was 25, 50, 75, and 100 mg/L. For optimization of contact time, samples were taken at predetermined time intervals (0–120 min) for determination of the residual metal ion concentration in the solution. Before analysis, the samples were centrifuged at 5000 rpm to separate the biomass. The residual metal concentrations in the supernatant were analyzed by FIAS-AAS.

The amount of the metal adsorbed (mg) per unit mass of biomatrix was obtained by using the equation:

$$q_e = (C_o - C_e) \times \frac{V}{m}, \quad (1)$$

where  $q_e$  is amount of metal ion adsorbed per gram of biomass ( $\text{mg} \cdot \text{g}^{-1}$ ),  $C_o$  is the initial metal ion concentration ( $\text{mg L}^{-1}$ ),  $C_e$  is the final metal ion concentration ( $\text{mg L}^{-1}$ ),  $V$  is the volume of the reaction mixture in liter, and  $m$  is the weight of biomass in the reaction mixture in g.

## 3. Results and Discussion

**3.1. Characterization of Adsorbent.** Fourier transform infrared (FTIR) spectroscopy was done to identify the chemical functional groups present on native ALP and the  $\text{Hg}(\text{II})$ -loaded ALP. The spectrum was collected by PU420, JASCO spectrometer in the range  $400\text{--}4,000 \text{ cm}^{-1}$  using a KBr window. The background obtained from the scan of pure KBr was automatically subtracted from the sample spectra. Spectra

were plotted using the same scale on the absorbance axis. Various functional groups such as amine ( $-NH$ ), carboxylate anions ( $-COO^-$ ), hydroxyl ( $-OH$ ), and others: ( $N=O$ ) ( $-C=C$ ), ( $-C-C$ ), ( $-C=O$ ), ( $-C-O$ ), ( $-C-N$ ), and ( $-C-H$ ) have been proposed to be responsible for the adsorption heavy metal ions on the cell surfaces of adsorbent. Their importance for metal uptake depends on factors such as the quantity of sites, its accessibility and chemical state, or affinity between site and metal. The FTIR absorption spectra of unloaded and Hg(II) loaded were taken (Figures 1(a) and 1(b)) to confirm the presence of different functional groups in adsorbent.

In the FTIR absorption, spectra of unloaded ALP biomass show a broadband at  $3438\text{ cm}^{-1}$  which indicates the presence of hydrogen-bonded  $-OH$  stretching modes from alcohol and phenols and also dominated by  $-NH$  stretching. The bands at  $2900$  and  $2853\text{ cm}^{-1}$  in IR spectra of ALP may be due to the  $C-H$  stretching vibrations. The peak at  $2329$  represents stretching vibrations of  $-NH_2^+$ ,  $-NH^+$ , and  $-NH$  groups of the unloaded ALP biomass. The bands appearing at  $1629$  and  $1380\text{ cm}^{-1}$  are attributed to the formation of oxygen functional groups like a highly conjugated  $C=O$  stretching in carboxylic groups and  $N=O$  bending in nitro groups, respectively. The peak appeared at  $1024\text{ cm}^{-1}$  has been assigned to  $C-O$  stretching in ethers. The peak at  $607\text{ cm}^{-1}$  is caused by  $C-N-C$  scissoring, which is found in polypeptide structure.

The small shift was obtained in the absorbance peak of loaded Hg(II) ALP biomass compared with that of unloaded ALP biomass which is shown in Figures 1(a) and 1(b). The broadband observed at  $3438\text{ cm}^{-1}$  for hydrogen-bonded  $-OH$  stretching and  $-NH$  stretching was shifted to  $3449\text{ cm}^{-1}$ . The peaks at  $2900$  and  $2853\text{ cm}^{-1}$  due to the  $C-H$  stretching vibrations were shifted to  $2924$  and  $2860\text{ cm}^{-1}$ , respectively. The stretching vibration band observed at  $2329\text{ cm}^{-1}$  was altered to  $2352\text{ cm}^{-1}$ . The peaks of highly conjugated  $C=O$  stretching and  $N=O$  bending observed at  $1629$  and  $1380\text{ cm}^{-1}$  were shifted to  $1646$  and  $1400\text{ cm}^{-1}$ .  $C-O$  stretching peak at  $1024\text{ cm}^{-1}$  was changed to  $1026\text{ cm}^{-1}$ . The  $C-N-C$  scissoring peak at  $607\text{ cm}^{-1}$  was also shifted to  $780\text{ cm}^{-1}$ . It should also be noted that FTIR results did not provide any quantitative analysis as well as the information about the level of affinity to metal of the functional groups presented in the adsorbents. They only presented the possibility of the coupling between the metal species and the functional group of the adsorbents.

The surface morphology of the ALP and Hg(II)-loaded ALP was analyzed by scanning electron microscopy (SEM) by using JEOL-JSM-6380 model which is shown in Figures 2(a) and 2(b). SEM micrograph of fresh ALP (Figure 2(a)) revealing the nature of biomass which is rough and heterogeneous with considerable amount of voids and lot of ups and downs. The uptake of Hg(II) by ALP is demonstrated by the change in morphology of the adsorbent's surface with the formation of-ike structure (Figure 2(b)). Based on the surface morphology results of ALP, it is suggested that produced ALP can be used as adsorbent for liquid-solid adsorption processes, due to the importance of fibrous material to many liquid-solid adsorption processes.

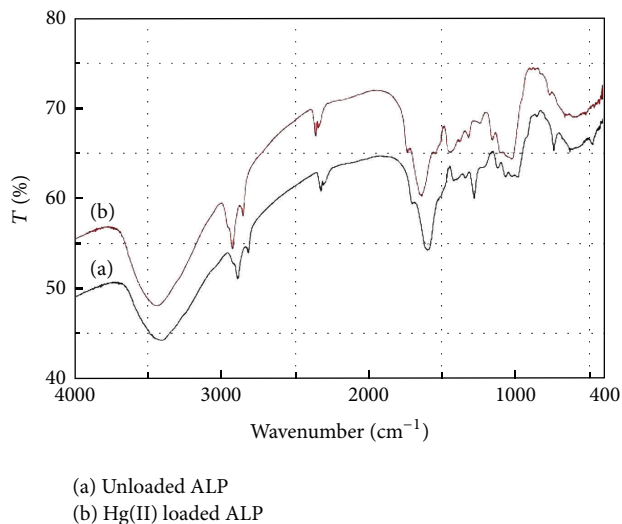


FIGURE 1: FTIR spectra's of (a) unloaded ALP and (b) Hg(II) loaded ALP.

**3.2. Effect of pH.** The effect of pH was found to be the most important variable governing the biosorption of metal ions by sorbent in the pH range of 3–9. Change in the removal of Hg(II) by ALP biomass with pH is shown in Figure 3. A significant increase in Hg(II) uptake was obtained as the pH increases from 3 to 6. The highest adsorption efficiency (97.5%) was observed at pH 6. At low pH value, more proton will be available to protonate the active sites and then less attraction towards the Hg(II) ions (low metal uptake) due to high electrostatic repulsion. When the pH was increased, the competing effect of  $H^+$  ion decreased and the positively charged Hg(II) ion took up the free active sites [45]. At pH greater than 6, the decrease in mercury (II) uptake occurs due to the formation of hydroxyl species such as  $[Hg(OH)]$  or  $Hg(OH)_2$ , and competing between mercury ions and hydroxyl species start, and  $OH^-$  occupies active sites of the adsorbent. Similar results have been reported by other researchers [34, 46–48].

**3.3. Effect of Biomass Concentration.** Amount of biomass used for the treatment studies is an important parameter, which determines the potential of adsorbent to remove mercury at a given initial concentration. The results clearly indicate the increase in Hg(II) uptake with increase in the biomass dosage from 0.25 to 1g and accomplished the equilibrium at 40 min of contact time. Removal of Hg(II) was found to increase proportionality with the amount of ALP biomass dose until reaching a constant (Figure 4). The increase in percentage removal of Hg(II) is expected with increase in adsorbent dosage as the number of active sites increases. Hence, higher dosage of adsorbent has positive effect on the initial rate of metal ion removal. However, increase in adsorbent dose at constant metal concentration and volume will lead to unsaturation of sorption sites, and metals ions are inadequate to cover all the redeemable sites [49, 50].

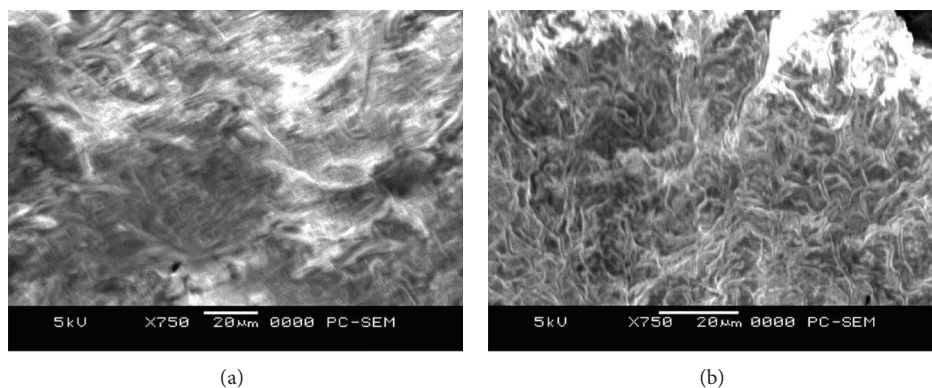


FIGURE 2: SEM of (a) unloaded ALP and (b) Hg(II) loaded ALP.

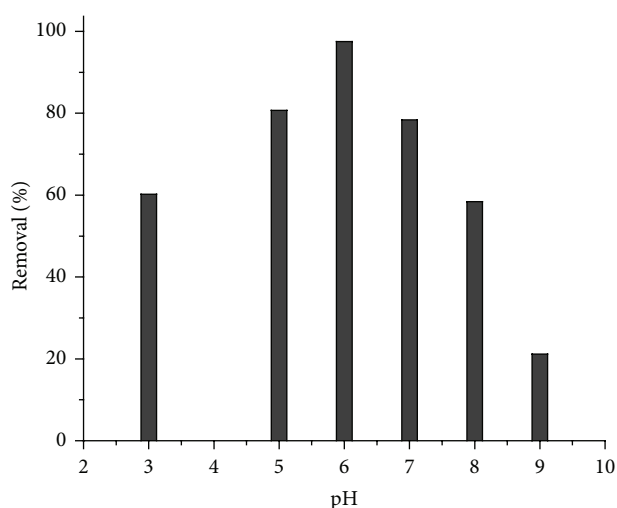


FIGURE 3: Effect of pH on the Hg(II) removal by ALP biomass.

At very low biomass concentration, the adsorbent surface becomes saturated with the metal ions, and the residual metal ion concentration in the solution is large. At 1 g/100 mL of biomass dosage, the Hg(II) uptake was found to be 97.5%, and this dose was taken as the optimum for further experiments.

**3.4. Effect of Initial Concentration with Time.** The rate of sorption is one of the most important parameters when designing a batch sorption experiment. The experimental runs measuring the effect of contact time on the biosorption of mercury at the different metal ion concentrations, 1.0 gm adsorbent dose, pH 6 and at 303 K. As shown in Figure 5, the biosorption of mercury was fast in the early stages, and the equilibrium adsorption was attained in 40 min of contact time. The observed fast biosorption kinetics is consistent with the biosorption of metal involving nonenergy-mediated reactions, where metal removal from solutions is purely due to physicochemical interactions between the biomass and the metal solution. The removal of Hg(II) increased from 23.7 mg/g to 65.1 mg/g sharply with time in the initial stage of 0–40 min range and then steady augmentation to

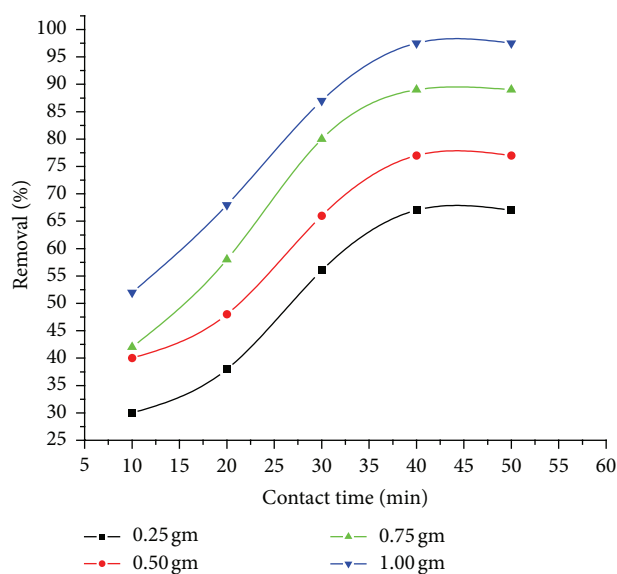


FIGURE 4: Effect of adsorbent dose with time on the removal of Hg(II) by ALP biomass.

attain equilibrium in just about 40 min time. Therefore, the optimum time and initial concentration for attaining the adsorption equilibrium is 40 min and 100 mg/L, respectively. It is perceived from the outcome that additional increase in the contact time has negligible effect on the sorption of metal ion. Many researchers have practiced the similar observation that Hg(II) removal increased almost linearly with the enhancement of the Hg(II) concentration [22, 34, 51, 52].

**3.5. Adsorption Isotherms.** The adsorption capacity and affinity of ALP for Hg(II) was determined with three isotherms models, namely, Langmuir, Freundlich and Temkin. The Langmuir model represents one of the first theoretical treatments of nonlinear sorption and suggests that uptake occurs on a homogeneous surface by monolayer sorption without interaction between adsorbed molecules. In addition, the



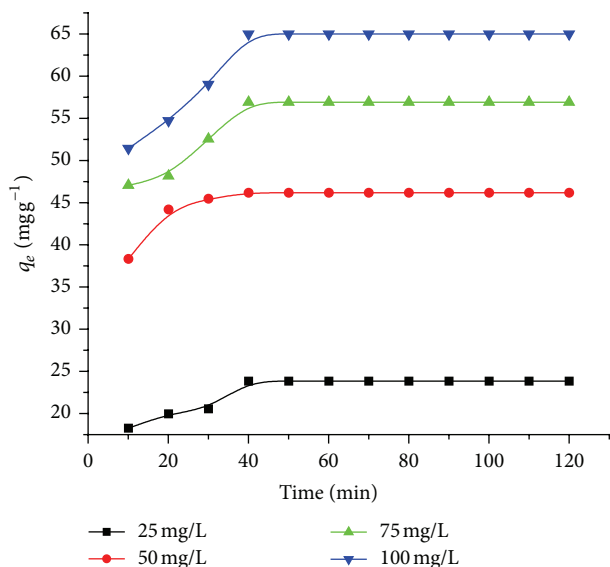


FIGURE 5: Effect of initial concentration and time on the sorption of Hg(II) at pH 6.0 and 1.0 g of Adulsa leaves powder.

model assumes uniform energies of adsorption onto the surface and no transmigration of the adsorbate. The Langmuir isotherm is represented in the following equation [33]:

$$q_e = \frac{q_m K_L C_e}{1 + K_L C_e} \quad (2)$$

Equation (2) is usually linearized to obtain the following form:

$$\frac{C_e}{q_e} = \frac{1}{K_L q_m} + \left( \frac{1}{q_m} \right) C_e \quad (3)$$

where  $C_e$  is the equilibrium concentration ( $\text{mg}\cdot\text{L}^{-1}$ ),  $q_e$  is the amount of adsorbed species per gram of adsorbent ( $\text{mg}\cdot\text{g}^{-1}$ ),  $K_L$  is the Langmuir equilibrium constant related to the energy or net enthalpy of adsorption, and  $q_m$  ( $\text{mg}\cdot\text{g}^{-1}$ ) is the amount of adsorbate required to complete monolayer coverage. The plot of  $C_e/q_e$  versus  $C_e$  was analyzed to find out the Langmuir isotherm parameters which are given in Table 1. From the results, it is shown that Langmuir plot (Figure 6) gives a good fit to the experimental data with coefficient of determination  $R^2 = 0.9909$ . The maximum biosorption capacity of ALP biomass for Hg(II) was found to be  $107.5 \text{ mg g}^{-1}$ . The value of adsorption energy,  $K_L$  was found to be  $0.0913 \text{ L mg}^{-1}$ .

The shape of the Langmuir isotherm can be expressed in terms of a dimensionless constant called separation factor or equilibrium parameter ( $R_L$ ), which is represented as

$$R_L = \frac{1}{1 + K_L C_o} \quad (4)$$

where  $C_o$  ( $\text{mg}\cdot\text{L}^{-1}$ ) is the initial concentration of the metal ion. If the average of the  $R_L$  values from the different initial concentrations used is between 0 and 1 ( $0 < R_L < 1$ ), it indicates favorable adsorption process; however, a  $R_L > 1$

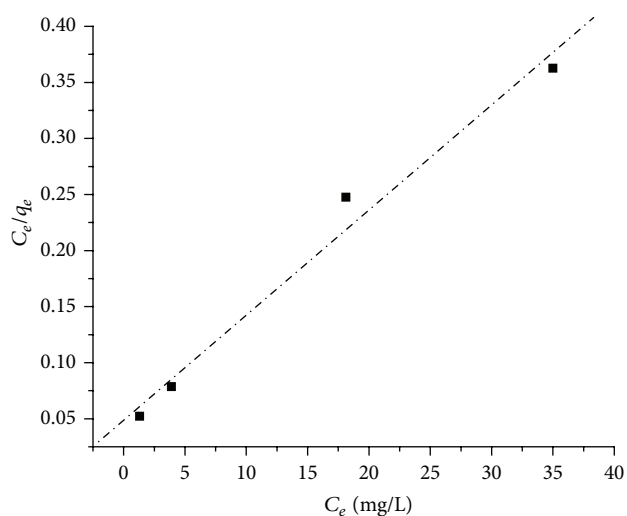


FIGURE 6: Langmuir isotherm model of Hg(II) sorption onto ALP biomass (at 303 K, pH 6.0).

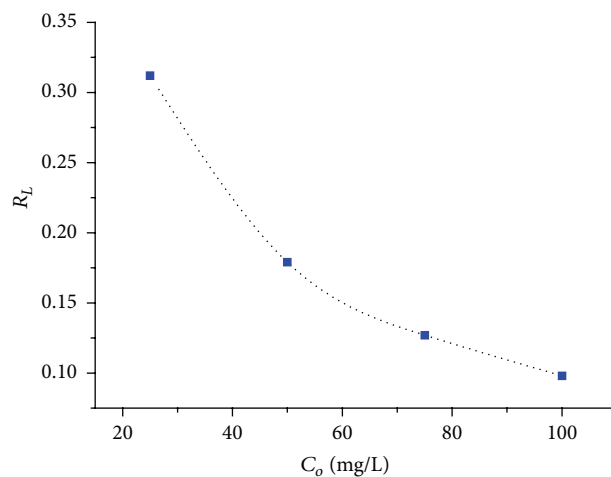


FIGURE 7: Separation factor for adsorption of Hg(II) by ALP biomass.

represents an unfavorable process. Alternatively, if  $R_L = 1$ , adsorption is linear. Lastly, if  $R_L = 0$ , the adsorption process is irreversible [53]. Figure 7 shows that  $0 < R_L < 0.05$  adsorption of Hg(II) onto ALP biomass. Because  $R_L$  is larger than zero, the adsorption process is considered favorable.

The Freundlich isotherm is a nonlinear sorption model. This model proposes a monolayer sorption with a heterogeneous energetic distribution of active sites, accompanied by interactions between adsorbed molecules. The general form of this model is [54]

$$q_e = K_F C_e^{1/n} \quad (5)$$

$$\ln q_e = \left( \frac{1}{n} \right) \ln C_e + \ln K_F,$$

where  $K_F$  and  $n$  are the Freundlich equilibrium constants related to the adsorption capacity and intensity of adsorption, respectively. The values of  $K_F$  and  $n$  were determined from

TABLE 1: Isotherms parameters for adsorption of Hg(II) onto ALP biomass at 303 K.

Langmuir model	$\frac{C_e}{q_e} = \frac{1}{K_L q_m} + \left(\frac{1}{q_m}\right) C_e$	$K_L$ (L/mg)	0.0913
		$q_m$ (mg/g)	1075
		$R^2$	0.990
Freundlich model	$\ln q_e = \left(\frac{1}{n}\right) \ln C_e + \ln K_F$	$K_F$ ((mg/g)/mg/L) <sup>1/n</sup>	1.32
		$n$	2.076
		$R^2$	0.940
Temkin model	$q_e = B \ln A + B \ln C_e$ $B = \frac{RT}{b}$	$A$ (L g)	7.39
		$B$ (KJ/mol)	0.2142
		$R^2$	0.973

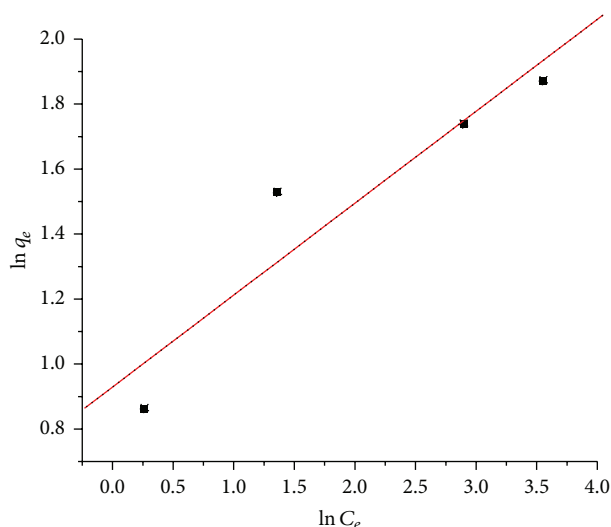


FIGURE 8: Freundlich isotherm model of Hg(II) sorption onto ALP biomass (at 303 K, pH 6.0).

a plot of  $\ln(q_e)$  versus  $\ln(C_e)$  as shown in Figure 8. The  $K_F$  constant in the Freundlich equilibrium was found to be 1.32 (mg/g)/mg/L)<sup>1/n</sup>. The value of  $n$  was between 0 and 10, suggesting relatively strong adsorption of these ions onto the surface of ALP biomass; for this study, we found a value of 2.076 for  $n$ . However, low correlation coefficients ( $R^2 = 0.940$ ) suggest that this was not the best model to describe these equilibria. Similar result for the magnitude of  $n$  was described by several researchers [55–57].

Temkin isotherm model considered the effects of indirect adsorbate-adsorbate interaction isotherms which explained that the heat of adsorption of all the molecules on the adsorbent surface layer would decrease linearly with coverage due to adsorbate-adsorbate interactions. Therefore, the adsorption potentials of the adsorbent for the adsorbate can be evaluated using Temkin adsorption isotherm model, which assumes that the fall in the heat of sorption is linear rather than logarithmic as implied in the Freundlich equation [58]. The Temkin isotherm can be given as

$$q_e = \left(\frac{RT}{b}\right) \ln AC_e. \quad (6)$$

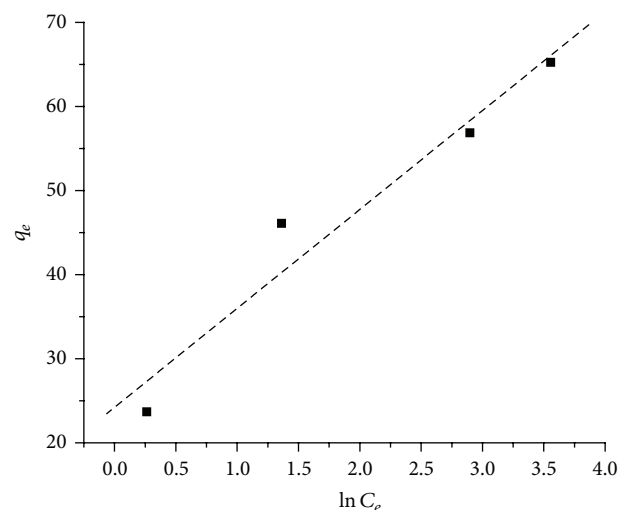


FIGURE 9: Temkin isotherm model of Hg(II) sorption onto ALP biomass (at 303 K, pH 6.0).

Equation (6) can be expressed in its linear form as

$$q_e = B \ln A + B \ln C_e, \quad (7)$$

with

$$B = \frac{RT}{b}, \quad (8)$$

where  $A$  is the equilibrium binding constant ( $L \cdot g^{-1}$ ),  $b$  (J/mol) is a constant related to heat of adsorption,  $R$  is the gas constant (8.314 J/mol/K), and  $T$  is the absolute temperature (K). As shown in Figure 9, the plot of  $q_e$  versus  $\ln C_e$  enables to determine the isotherm constants  $A$ ,  $b$  from the slope and intercept, respectively. The correlation coefficient  $R^2 = 0.973$  for the adsorption of Hg(II) ion in temkin isotherm was fairly fitted well as compared to the Freundlich isotherm. The experimental and theoretical adsorption capacity was calculated from isotherm models. The calculated parameters for all the isotherms are accessible in Table 1. The best-fit experimental equilibrium data derived from the Langmuir model suggested that the monolayer coverage and chemisorption of Hg(II) onto ALP.

3.6. *Biosorption Kinetics.* Lagergren's pseudofirst-order [59] and Ho's pseudosecond-order models [60] were applied to the experimental data in order to clarify the biosorption kinetics of Hg(II) ions onto ALP. The expression for the pseudofirst-order by Lagergren is given by the differential rate law:

$$\frac{dq_t}{dt} = k_1 (q_e - q_t), \quad (9)$$

where  $q_e$  is the amount of solute adsorbed at equilibrium per unit weight of adsorbent ( $\text{mg g}^{-1}$ ),  $q_t$  ( $\text{mg g}^{-1}$ ) is the amount of the metal ion bioadsorbed at equilibrium and time  $t$ , and  $k_1$  ( $\text{min}^{-1}$ ) is the adsorption constant. Equation (9) was integrated under the boundary conditions, giving a linear expression:

$$\ln(q_e - q_t) = \ln q_e - k_1 t. \quad (10)$$

The linear plot of  $\ln(q_e - q_t)$  versus  $t$  shows the applicability of Lagergren equation which is shown in Figure 10. The value-of  $k_1$  and  $q_e$  calculated from the linear pseudofirst-order kinetic model and the corresponding correlation coefficients ( $R^2$ ) are summarized in Table 2. The correlation coefficient for the pseudofirst-order kinetic model obtained at the studied optimum condition was 0.983.

The expression for the pseudosecond-order model is given by the differential rate law:

$$\frac{dq_t}{dt} = k_2 (q_e - q_t)^2 \quad (11)$$

which is on integration under the boundary conditions of  $t = 0$  to  $t > 0$  and  $q_t = 0$  to  $q_t > 0$ , and after rearranging (11), the following linearized form of the pseudosecond-order model was obtained:

$$\frac{t}{q_t} = \frac{1}{(k_2 q_e^2)} + \left(\frac{1}{q_e}\right) t. \quad (12)$$

The initial adsorption rate ( $h$ ) can be determined from  $k_2$  and  $q_e$  values using

$$h = k_2 q_e^2, \quad (13)$$

where  $k_2$  is the rate constant of the pseudosecond-order sorption ( $\text{g mg}^{-1} \text{min}^{-1}$ ) which can be obtained by plot of  $t/q_t$  against  $t$ . The rate constant  $k_2$  and equilibrium amount of metal ion  $q_e$  can be determined from slope and intercept of the plot (Figure 11). The values of  $k_2$ ,  $q_e$  and the initial adsorption rate ( $h$ ) were calculated as  $2 \times 10^{-3} \text{ g mg}^{-1} \text{ min}^{-1}$ ,  $46.6 \text{ mg g}^{-1}$ , and  $4.34 \text{ mg g}^{-1} \text{ min}^{-1}$ , respectively. The correlation coefficient for the pseudosecond order was 0.998. The excellent linearity and high value of correlation coefficient ( $R^2$ ) from Figure 11 shows that the process follows the pseudosecond-order model with good fit in comparison to pseudofirst order model. This suggests that sorption of the metal ions involve two species in this case, the metal ion and the biomass. These results are in accordance with similar works on other metal ions [61–63] with several other natural sorbents.

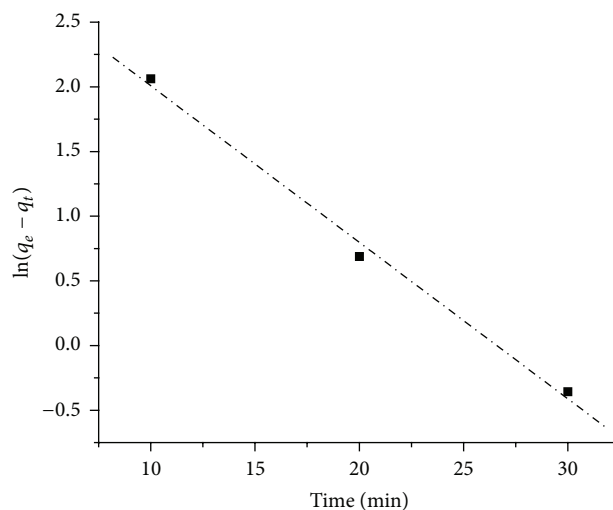


FIGURE 10: Lagergren plot for the adsorption of Hg(II) ions by ALP biomass at pH 6.

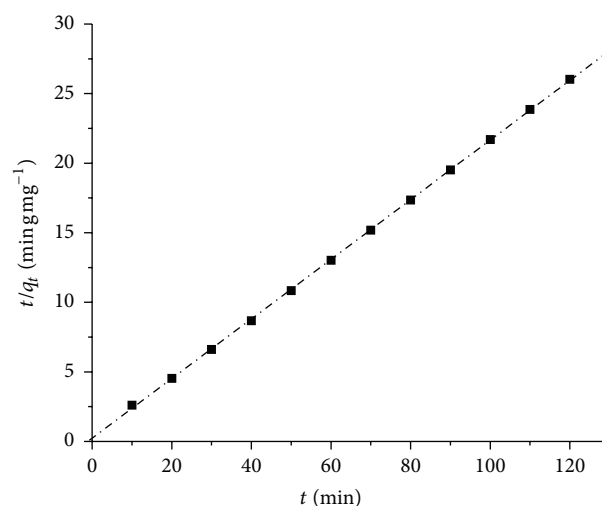


FIGURE 11: Pseudosecond-order kinetics for the adsorption of Hg(II) by ALP biomass at pH 6.

3.6.1. *Elovich Kinetic Model.* The Elovich kinetic model is for general application to chemisorption kinetics. The general explanation for this form of kinetic law involves that the active sites are heterogeneous in nature and therefore exhibit different activation energies for chemisorptions. The Elovich model can be expressed in the following form [64]:

$$\frac{dq_t}{dt} = \alpha \exp(-\beta q_t). \quad (14)$$

To simplify the above equation, assume  $\alpha\beta \gg 1$  [65], and by applying the boundary conditions  $q_t = 0$  at  $t = 0$  and  $q_t = q_t$  at  $t = t$ , (14) becomes [66]

$$q_t = \beta \ln(\alpha \beta) + \ln t, \quad (15)$$

where  $q_t$  is the adsorption capacity at time  $t$  ( $\text{mg g}^{-1}$ ),  $\alpha$  is the initial adsorption rate ( $\text{mg g}^{-1} \text{ min}^{-1}$ ) and  $\beta$  is the desorption

TABLE 2: Kinetic parameters for adsorption of Hg(II) onto ALP biomass at 303 K.

Kinetic model	Linear equation	Reaction constant	$q_e$ (mg/g)	$R^2$
Pseudofirst order	$\ln(q_e - q_t) = \ln q_e - k_1 t$	$K_1 = 0.1209 \text{ min}^{-1}$	32.1	0.983
Pseudosecond order	$\frac{t}{q_t} = \frac{1}{(k_2 q_e^2)} + \left(\frac{1}{q_e}\right)t$	$K_2 = 2 \times 10^{-3} \text{ g/mg min}$ $h = 4.34 \text{ mg/g}\cdot\text{min}$	46.6	0.998
Elovich	$q_t = \beta \ln(\alpha\beta) + \ln(t)$	$B = 5.86 \text{ g/mg}$ $A = 38 \text{ mg/g}\cdot\text{min}$	—	0.9661
Intraparticle diffusion	$q_t = K_{id} t^{1/2}$	$K_{id} = 1.70 \text{ mg/g}\cdot\text{min}^{0.5}$ $I = 3.1029$	—	0.9152

constant ( $\text{g}\cdot\text{mg}^{-1}$ ), which are obtained from the intercept and the slope of a plot of  $q_t$  versus  $\ln t$ . The plot should give a linear relationship for the applicability of simple Elovich kinetics as in Figure 12. The correlation coefficient  $R^2$  is obtained as 0.9661 for Hg(II) ions which is found to be less than the values calculated using pseudofirst-order kinetic model and pseudosecond-order kinetic model as shown in Table 2. The calculated reaction constants  $\alpha$  and  $\beta$  were found  $5.86 \text{ g}\cdot\text{mg}^{-1}$  and  $38 \text{ mg}\cdot\text{g}^{-1}\cdot\text{min}^{-1}$ , respectively.

**3.6.2. Intraparticle Diffusion.** The adsorbate transport from the solution phase to the surface of the adsorbent particles occurs in several steps. The overall adsorption process may be controlled either by one or more steps, for example, film or external diffusion, pore diffusion, surface diffusion, and the adsorption on the pore surface or a combination of more than one steps. The adsorption rate parameter which controls the batch process for most of the contact time is the intraparticle diffusion. Good linearization of the data is observed for the initial phase of the reaction in accordance with the expected behavior if intraparticle diffusion is the rate-limiting step [67]. The possibility of intraparticle diffusion was explored by using Weber and Morris equation:

$$q_t = K_{id} t^{1/2} + I. \quad (16)$$

The slope and intercept of plot  $q_t$  versus  $t^{1/2}$  were used to calculate the intraparticle diffusion rate constant,  $K_{id}$  ( $\text{mg}\cdot\text{g}^{-1}\cdot\text{min}^{0.5}$ ). Values of  $I$  give an idea about the thickness of the boundary layer; that is, the larger the intercept, the greater is the boundary layer effect. The deviation of straight lines from the origin, as shown in the Figure 13, may be because of the difference between the rate of mass transfer in the initial and final steps of adsorption. Further, such deviation of straight line from the origin indicates that the pore diffusion is not the sole rate-controlling step [68]. It can also be concluded on the basis of  $I$  value as  $I \neq 0$  thus suggesting that intraparticle diffusion is not the rate-limiting step. The correlation coefficient ( $R^2 = 0.9152$ ) value was calculated from the respective plot and provided in Table 2. The value of the correlation coefficient was not uniform or large enough to suggest that intraparticle diffusion is the rate determining step of the adsorption process. The intraparticle diffusion rate constant ( $K_{id}$ ) and thickness of the boundary layer ( $I$ ) values were  $1.70 \text{ mg}\cdot\text{g}^{-1}\cdot\text{min}^{0.5}$  and 3.1029, respectively.

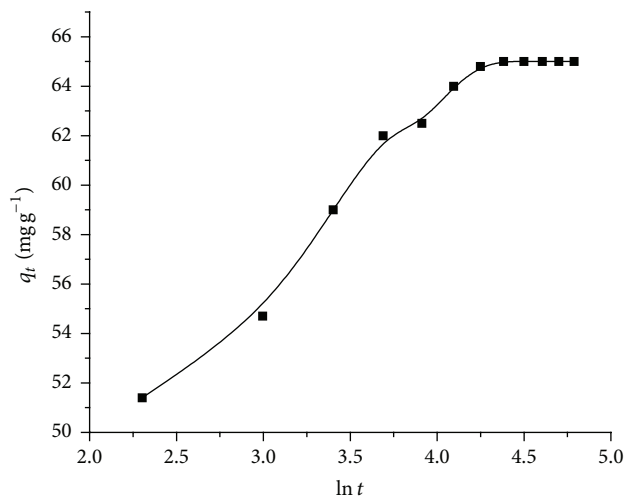


FIGURE 12: Elovich kinetic model for the adsorption of Hg(II) onto ALP biomass.

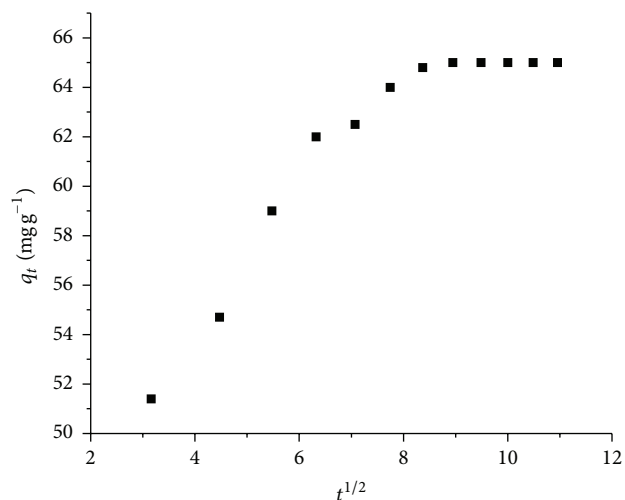


FIGURE 13: Intraparticle diffusion of Hg(II) adsorption onto ALP biomass.

#### 4. Comparison of the Present Study with Literature

Table 3 shows various adsorbents previously studied for Hg(II) removal. Although the data collected in this table may



TABLE 3: Comparison of monolayer maximum adsorption capacity of Hg(II) ion with various adsorbents.

Biosorbents	$q_m$ (mg g <sup>-1</sup> )	References
Wheat bran	70.0	[21]
Waste rubber	4.0	[24]
<i>Eucalyptus</i> bark	33.1	[18]
Coir pith	154	[31]
Furfural	174	[33]
Walnut shell	151.51	[22]
Peanut hull	110	[28]
<i>Carica papaya</i>	155.6	[19]
Sago waste	55.6	[32]
Fruit shell of <i>Terminalia catappa</i>	94.4	[34]
Adulsa ( <i>Justicia Adhatoda</i> ) leaves powder	107.5	Present study
Polyaniline/attapulgit	800	[35]
Moss	94.4	[36]
Malt spent rootless	50	[37]
Acrylic textile fibre	290–710	[38]
<i>Potamogeton natans</i>	180	[39]
Macroalgae	329	[40]
Fertilizer waste	$3.62 \times 10^{-3}$	[41]
Camel bone charcoal	28.2	[42]
Garlic ( <i>Allium sativum</i> L.)	0.6497	[43]
Carbon aerogel	34.96	[44]

or may not represents equivalent or optimized conditions or various mercury removal mechanisms in each case, it still provides a useful comparison regarding decision of selection of suitable adsorbent. The maximum adsorption capacity of mercury by ALP biomass in this study is comparable with these data. Indeed mercury adsorption by ALP biomass in this study was significantly higher than most of the selected biomass.

## 5. Conclusions

The study shows that Adulsa leaves can be used as a sorbent for the removal of Hg(II) ions from aqueous media. FTIR data confirmed that the functional groups such as hydroxyl, carboxyl, and amine groups were responsible for the adsorption of Hg(II) ion onto ALP biomass. Under batch condition, equilibrium was attained within 40 min. The amount of metal removal at equilibrium (40 min) increases from 67 to 97.5% with an increase of adsorbent dosage between 0.25 and 1 gm. On changing the initial concentration from 25 to 100 mg/L, the amount of mercury adsorbed increased from 23.7 to 65 mg/g at 303 K for a period of 40 min. The Langmuir isotherm that described the adsorption of Hg(II) ions onto the ALP biomass ( $R^2 = 0.990$ ) was better than the freundlich model ( $R^2 = 0.940$ ) and the temkin model ( $R^2 = 0.973$ ). The study demonstrated that under optimum conditions (pH = 6.0, biomass dosage = 1 gm, temperature = 303 K, and contact time = 40 min), maximum adsorption capacity for Hg(II) was found to be 107.5 mg/g from Langmuir isotherm. Pseudosecond-order kinetics explained the adsorption of

metal ion better than the pseudofirst order.  $K_{id}$  indicates that the pore diffusion is not the sole rate-controlling step. Furthermore, it can be concluded that Adulsa leaves powder hold great potential to be an environmentally friendly effective adsorbent for the removal of mercury ions from contaminated waters.

## References

- [1] F. M. M. Morel, A. M. L. Kraepiel, and M. Amyot, "The chemical cycle and bioaccumulation of mercury," *Annual Review of Ecology and Systematics*, vol. 29, pp. 543–566, 1998.
- [2] R. Baeyens, R. Ebinghous, and O. Vasilev, *Global and Regional Mercury Cycles: Sources, Fluxes and Mass Balances*, Kluwer Academic, 1996.
- [3] D. W. Boening, "Ecological effects, transport, and fate of mercury: a general review," *Chemosphere*, vol. 40, no. 12, pp. 1335–1351, 2000.
- [4] N. Pirrone, S. Cinnirella, X. Feng et al., "Global mercury emissions to the atmosphere from anthropogenic and natural sources," *Atmospheric Chemistry and Physics*, vol. 10, no. 13, pp. 5951–5964, 2010.
- [5] S. Innanen, "The ratio of anthropogenic to natural mercury release in Ontario: three emission scenarios," *Science of the Total Environment*, vol. 213, no. 1–3, pp. 25–32, 1998.
- [6] T. Morimoto, S. Wu, M. Azhar Uddin, and E. Sasaoka, "Characteristics of the mercury vapor removal from coal combustion flue gas by activated carbon using H<sub>2</sub>S," *Fuel*, vol. 84, no. 14–15, pp. 1968–1974, 2005.
- [7] Y. H. Li, C. W. Lee, and B. K. Gullett, "Importance of activated carbon's oxygen surface functional groups on elemental mercury adsorption," *Fuel*, vol. 82, no. 4, pp. 451–457, 2003.
- [8] F. Di Natale, A. Lancia, A. Molino, M. Di Natale, D. Karatza, and D. Musmarra, "Capture of mercury ions by natural and industrial materials," *Journal of Hazardous Materials*, vol. 132, no. 2–3, pp. 220–225, 2006.
- [9] WHO, UNEP, "Guidance for Identifying Populations at Risk from Mercury Exposure, UNEP DTIE Chemicals Branch and WHO Department of Food Safety," *Zoonoses and Foodborne Diseases*, p. 4, 2008.
- [10] R. H. Crist, J. R. Martin, J. Chonko, and D. R. Crist, "Uptake of metals on peat moss: an ion-exchange process," *Environmental Science and Technology*, vol. 30, no. 8, pp. 2456–2461, 1996.
- [11] C. P. Huang and D. W. Blankenship, "The removal of mercury (II) from dilute aqueous solution by activated carbon," *Water Research*, vol. 18, no. 1, pp. 37–46, 1984.
- [12] H. K. Alluri, S. R. Ronda, V. S. Settalluri, B. Jayakumar Singh, V. Suryanarayana, and P. Venkateshwar, "Biosorption: an eco-friendly alternative for heavy metal removal," *African Journal of Biotechnology*, vol. 6, no. 25, pp. 2924–2931, 2007.
- [13] B. Volesky and Z. R. Holan, "Biosorption of heavy metals," *Biotechnology Progress*, vol. 11, no. 3, pp. 235–250, 1995.
- [14] B. Volesky, "Detoxification of metal-bearing effluents: biosorption for the next century," *Hydrometallurgy*, vol. 59, no. 2–3, pp. 203–216, 2001.
- [15] B. S. Marina, M. P. Jelena, and N. R. Radojka, "Biosorption of copper(ii) and chromium(vi) by modified tea Fungus," *APTEFF*, vol. 43, pp. 1–342, 2012.
- [16] Y. Nuhoglu and E. Malkoc, "Thermodynamic and kinetic studies for environmentally friendly Ni(II) biosorption using

- waste pomace of olive oil factory," *Bioresource Technology*, vol. 100, no. 8, pp. 2375–2380, 2009.
- [17] A. Khanafari, S. Eshghdoost, and A. Mashinchian, "Removal of lead and chromium from aqueous solution by *Bacillus circulans* biofilm," *Iranian Journal of Environmental Health Science and Engineering*, vol. 5, no. 3, pp. 195–200, 2008.
- [18] I. Ghodbane and O. Hamdaoui, "Removal of mercury(II) from aqueous media using eucalyptus bark: kinetic and equilibrium studies," *Journal of Hazardous Materials*, vol. 160, no. 2-3, pp. 301–309, 2008.
- [19] S. Basha, Z. V. P. Murthy, and B. Jha, "Sorption of Hg(II) onto *Carica papaya*: experimental studies and design of batch sorber," *Chemical Engineering Journal*, vol. 147, no. 2-3, pp. 226–234, 2009.
- [20] F. Rozada, M. Otero, A. Morán, and A. I. García, "Adsorption of heavy metals onto sewage sludge-derived materials," *Biore-source Technology*, vol. 99, no. 14, pp. 6332–6338, 2008.
- [21] M. A. Farajzadeh and A. B. Monji, "Adsorption characteristics of wheat bran towards heavy metal cations," *Separation and Purification Technology*, vol. 38, no. 3, pp. 197–207, 2004.
- [22] M. Zabihi, A. Ahmadvpour, and A. Haghighi Asl, "Removal of mercury from water by carbonaceous sorbents derived from walnut shell," *Journal of Hazardous Materials*, vol. 167, no. 1–3, pp. 230–236, 2009.
- [23] G. Macchi, D. Marani, and G. Tiravanti, "Uptake of mercury by exhausted coffee grounds," *Environmental Technology Letters*, vol. 7, no. 8, pp. 431–444, 1986.
- [24] W. R. Knocke and L. H. Hemphill, "Mercury(II) sorption by waste rubber," *Water Research*, vol. 15, no. 2, pp. 275–282, 1981.
- [25] M. K. Sreedhar, A. Madhukumar, and T. S. Anirudhan, "Evaluation of an adsorbent prepared by treating coconut husk with polysulphide for the removal of mercury from wastewater," *Indian Journal of Engineering and Materials Sciences*, vol. 6, no. 5, pp. 279–285, 1999.
- [26] S. K. Srivastava, R. Tyagi, and N. Pant, "Adsorption of heavy metal ions on carbonaceous material developed from the waste slurry generated in local fertilizer plants," *Water Research*, vol. 23, no. 9, pp. 1161–1165, 1989.
- [27] B. Volesky, "Removal and recovery of heavy metals by biosorption," in *Biosorption of Heavy Metals*, B. Volesky, Ed., pp. 7–43, CRC Press, Boca Raton, Fla, USA, 1990.
- [28] C. Namasivayam and K. Periasamy, "Bicarbonate-treated peanut hull carbon for mercury (II) removal from aqueous solution," *Water Research*, vol. 27, no. 11, pp. 1663–1668, 1993.
- [29] B. S. Inbaraj and N. S. Sulochana, "Utilization of an agricultural waste jack fruit peel for the removal of Hg(II) from aqueous solution," in *Proceeding of 17th International Conference on Solid Waste Technology and Management*, R. L. Mersky, Ed., pp. 802–811, Philadelphia, Pa, USA, 2001.
- [30] A. K. Sen and A. K. De, "Adsorption of mercury(II) by coal fly ash," *Water Research*, vol. 21, no. 8, pp. 885–888, 1987.
- [31] C. Namasivayam and K. Kadirvelu, "Uptake of mercury (II) from wastewater by activated carbon from an unwanted agricultural solid by-product: coirpith," *Carbon*, vol. 37, no. 1, pp. 79–84, 1999.
- [32] K. Kadirvelu, M. Kavipriya, C. Karthika, N. Vennilamani, and S. Pattabhi, "Mercury (II) adsorption by activated carbon made from sago waste," *Carbon*, vol. 42, no. 4, pp. 745–752, 2004.
- [33] I. Langmuir, "The constitution and fundamental properties of solids and liquids. Part I. Solids," *The Journal of the American Chemical Society*, vol. 38, no. 2, pp. 2221–2295, 1916.
- [34] B. S. Inbaraj and N. Sulochana, "Mercury adsorption on a carbon sorbent derived from fruit shell of *Terminalia catappa*," *Journal of Hazardous Materials*, vol. 133, no. 1–3, pp. 283–290, 2006.
- [35] H. Cui, Y. Qian, Q. Li, Q. Zhang, and J. Zhai, "Adsorption of aqueous Hg(II) by a polyaniline/attapulgite composite," *Chemical Engineering Journal*, vol. 211–212, pp. 216–223, 2012.
- [36] A. Sari and M. Tuzen, "Removal of mercury(II) from aqueous solution using moss (*Drepanocladus revolvens*) biomass: equilibrium, thermodynamic and kinetic studies," *Journal of Hazardous Materials*, vol. 171, no. 1–3, pp. 500–507, 2009.
- [37] V. A. Anagnostopoulos, I. D. Manariotis, H. K. Karapanagioti, and C. V. Chrysikopoulos, "Removal of mercury from aqueous solutions by malt spent rootlets," *Chemical Engineering Journal*, vol. 213, pp. 135–141, 2012.
- [38] J. V. Nabais, P. J. M. Carrott, M. M. L. R. Carrott et al., "Mercury removal from aqueous solution and flue gas by adsorption on activated carbon fibres," *Applied Surface Science*, vol. 252, no. 17, pp. 6046–6052, 2006.
- [39] C. Lacher and R. W. Smith, "Sorption of Hg(II) by *Potamogeton natans* dead biomass," *Minerals Engineering*, vol. 15, no. 3, pp. 187–191, 2002.
- [40] R. Herrero, P. Lodeiro, C. Rey-Castro, T. Vilariño, and M. E. Sastre De Vicente, "Removal of inorganic mercury from aqueous solutions by biomass of the marine macroalga *Cystoseira baccata*," *Water Research*, vol. 39, no. 14, pp. 3199–3210, 2005.
- [41] D. Mohan, V. K. Gupta, S. K. Srivastava, and S. Chander, "Kinetics of mercury adsorption from wastewater using activated carbon derived from fertilizer waste," *Colloids and Surfaces A*, vol. 177, no. 2-3, pp. 169–181, 2001.
- [42] S. S. M. Hassan, N. S. Awwad, and A. H. A. Aboterika, "Removal of mercury(II) from wastewater using camel bone charcoal," *Journal of Hazardous Materials*, vol. 154, no. 1–3, pp. 992–997, 2008.
- [43] Y. Eom, J. H. Won, J.-Y. Ryu, and T. G. Lee, "Biosorption of mercury(II) ions from aqueous solution by garlic (*Allium sativum* L.) powder," *Korean Journal of Chemical Engineering*, vol. 28, no. 6, pp. 1439–1443, 2011.
- [44] K. Kadirvelu, J. Goel, and C. Rajagopal, "Sorption of lead, mercury and cadmium ions in multi-component system using carbon aerogel as adsorbent," *Journal of Hazardous Materials*, vol. 153, no. 1-2, pp. 502–507, 2008.
- [45] S. Schiewer and B. Volesky, "Biosorption process for heavy metal removal," in *Environmental Microbe-Metal Interactions*, D. R. Lovley, Ed., pp. 329–362, ASM Press, Washington, DC, USA, 2000.
- [46] M. Amini, H. Younesi, N. Bahramifar et al., "Application of response surface methodology for optimization of lead biosorption in an aqueous solution by *Aspergillus niger*," *Journal of Hazardous Materials*, vol. 154, no. 1–3, pp. 694–702, 2008.
- [47] G. Bayramoğlu, I. Tuzun, G. Celik, M. Yilmaz, and M. Y. Arica, "Biosorption of mercury(II), cadmium(II) and lead(II) ions from aqueous system by microalgae *Chlamydomonas reinhardtii* immobilized in alginate beads," *International Journal of Mineral Processing*, vol. 81, no. 1, pp. 35–43, 2006.
- [48] Y. Zeroual, A. Moutaouakkil, F. Z. Dzairi et al., "Biosorption of mercury from aqueous solution by *Ulva lactuca* biomass," *Bioresource Technology*, vol. 90, no. 3, pp. 349–351, 2003.
- [49] R. Gong, Y. Ding, H. Liu, Q. Chen, and Z. Liu, "Lead biosorption and desorption by intact and pretreated spirulina maxima biomass," *Chemosphere*, vol. 58, no. 1, pp. 125–130, 2005.

- [50] N. Saifuddin and A. Z. Raziah, "Removal of heavy metals from industrial effluent using *Saccharomyces cerevisiae* (Baker's yeast) immobilized in chitosan/lignosulphonate matrix," *Journal of Applied Science Research*, vol. 3, pp. 2091–2099, 2007.
- [51] F.-S. Zhang, J. O. Nriagu, and H. Itoh, "Photocatalytic removal and recovery of mercury from water using TiO<sub>2</sub>-modified sewage sludge carbon," *Journal of Photochemistry and Photobiology A*, vol. 167, no. 2-3, pp. 223–228, 2004.
- [52] M. F. Yardim, T. Budinova, E. Ekinici, N. Petrov, M. Razvigorova, and V. Minkova, "Removal of mercury (II) from aqueous solution by activated carbon obtained from furfural," *Chemosphere*, vol. 52, no. 5, pp. 835–841, 2003.
- [53] W. S. Wan Ngah, A. Kamari, and Y. J. Koay, "Equilibrium and kinetics studies of adsorption of copper (II) on chitosan and chitosan/PVA beads," *International Journal of Biological Macromolecules*, vol. 34, no. 3, pp. 155–161, 2004.
- [54] H. M. F. Freundlich, "Über die adsorption in lasugen," *Zeitschrift Für Physikalische Chemie (Leipzig)*, vol. 57A, pp. 385–470, 1906.
- [55] Y.-M. Hao, C. Man, and Z.-B. Hu, "Effective removal of Cu (II) ions from aqueous solution by amino-functionalized magnetic nanoparticles," *Journal of Hazardous Materials*, vol. 184, no. 1–3, pp. 392–399, 2010.
- [56] T. K. Naiya, A. K. Bhattacharya, and S. K. Das, "Adsorption of Cd(II) and Pb(II) from aqueous solutions on activated alumina," *Journal of Colloid and Interface Science*, vol. 333, no. 1, pp. 14–26, 2009.
- [57] J. Hu, G. Chen, and I. M. C. Lo, "Removal and recovery of Cr(VI) from wastewater by maghemite nanoparticles," *Water Research*, vol. 39, no. 18, pp. 4528–4536, 2005.
- [58] M. I. Temkin and V. Pyzhev, "Kinetics of ammonia synthesis on promoted iron catalysts," *Acta Physicochimica URSS*, vol. 12, pp. 327–356, 1940.
- [59] S. Lagergren, *Zur Theorie Der Sogenannten Adsorption Geloster Stoffe*, vol. 24, Kungliga Sevenska Vetanskapas akademien, Handlingar, 1898.
- [60] Y. S. Ho and G. McKay, "Pseudo-second order model for sorption processes," *Process Biochemistry*, vol. 34, no. 5, pp. 451–465, 1999.
- [61] Y. Prasanna Kumar, P. King, and V. S. R. K. Prasad, "Equilibrium and kinetic studies for the biosorption system of copper(II) ion from aqueous solution using *Tectona grandis* L.f. leaves powder," *Journal of Hazardous Materials*, vol. 137, no. 2, pp. 1211–1217, 2006.
- [62] A. Lodi, C. Solisio, A. Converti, and M. Del Borghi, "Cadmium, zinc, copper, silver and chromium(III) removal from wastewaters by *Sphaerotilus natans*," *Bioprocess Engineering*, vol. 19, no. 3, pp. 197–203, 1998.
- [63] Y.-S. Ho, W.-T. Chiu, C.-S. Hsu, and C.-T. Huang, "Sorption of lead ions from aqueous solution using tree fern as a sorbent," *Hydrometallurgy*, vol. 73, no. 1-2, pp. 55–61, 2004.
- [64] M. J. D. Low, "Kinetics of chemisorption of gases on solids," *Chemical Reviews*, vol. 60, no. 3, pp. 267–312, 1960.
- [65] S. H. Chien and W. R. Clayton, "Application of Elovich equation to the kinetics of phosphate release and sorption in soils," *Soil Science Society of America Journal*, vol. 44, pp. 265–268, 1980.
- [66] D. L. Sparks, *Kinetics of Reaction in Pure and Mixed Systems*, Soil Phy Chem CRC Press, Boca Raton, Fla, USA, 1986.
- [67] W. J. Weber and J. C. Morris, "Kinetics of adsorption on carbon from solution," *Journal of the Sanitary Engineering Division, American Society of Civil Engineers*, vol. 89, pp. 31–60, 1963.
- [68] S. C. Ibrahim, M. A. K. M. Hanafiah, and M. Z. A. Yahya, "Removal of Cadmium form aqueous solutions by adsorption on sugarcane bagasse," *American European Journal of Agricultural & Environmental Sciences*, vol. 1, no. 3, pp. 179–184, 2006.



# The Scientific World Journal

Hindawi Publishing Corporation  
<http://www.hindawi.com>

Volume 2013



Hindawi

- ▶ Impact Factor **1.730**
- ▶ **28 Days** Fast Track Peer Review
- ▶ All Subject Areas of Science
- ▶ Submit at <http://www.tswj.com>